# A NONCONFORMING PENALTY METHOD FOR A TWO DIMENSIONAL CURL-CURL PROBLEM

SUSANNE C. BRENNER, FENGYAN LI, AND LI-YENG SUNG

Abstract. A nonconforming penalty method for a two-dimensional curl-curl problem is studied in this paper. It uses weakly continuous $P_1$ vector fields and penalizes the local divergence. Two consistency terms involving the jumps of the vector fields across element boundaries are also included to ensure the convergence of the scheme. Optimal convergence rates (up to an arbitrary positive $\epsilon$) in both the energy norm and the $L_2$ norm are established on graded meshes. This scheme can also be used in the computation of Maxwell eigenvalues without generating spurious eigenmodes. The theoretical results are confirmed by numerical experiments.

## 1. Introduction

Let $\Omega \subset \mathbb{R}^2$ be a bounded polygonal domain. We consider the following curl-curl problem in this paper.

Find $\mathring{\boldsymbol{u}} \in H_0(\mathrm{curl};\Omega) \cap H(\mathrm{div}^0;\Omega)$ such that

$$(\nabla \times \mathring{\boldsymbol{u}}, \nabla \times \boldsymbol{v}) + \alpha(\mathring{\boldsymbol{u}}, \boldsymbol{v}) = (\boldsymbol{f}, \boldsymbol{v}) \tag{1.1}$$

for all $\boldsymbol{v} \in H_0(\mathrm{curl};\Omega) \cap H(\mathrm{div}^0;\Omega)$, where $\boldsymbol{f} \in [L_2(\Omega)]^2$ and $(\cdot,\cdot)$ denotes the inner product of $[L_2(\Omega)]^2$. Here the function spaces $H_0(\mathrm{curl};\Omega)$ and $H(\mathrm{div}^0;\Omega)$ are defined by

$$H(\mathrm{curl};\Omega) = \Big\{\boldsymbol{v} = \begin{bmatrix} v_1 \\ v_2 \end{bmatrix} \in [L_2(\Omega)]^2 : \nabla \times \boldsymbol{v} = \frac{\partial v_2}{\partial x_1} - \frac{\partial v_1}{\partial x_2} \in L_2(\Omega)\Big\},$$
$$H_0(\mathrm{curl};\Omega) = \{\boldsymbol{v} \in H(\mathrm{curl};\Omega) : \boldsymbol{n} \times \boldsymbol{v} = 0\},$$

1991 *Mathematics Subject Classification.* 65N30, 65N15, 35Q60.

*Key words and phrases.* curl-curl problem, Maxwell equations, Maxwell eigenvalues, nonconforming finite element method.

The work of the first author was supported in part by the National Science Foundation under Grant Nos. DMS-03-11790 and DMS-07-13835, and by the Alexander von Humboldt Foundation through her Humboldt Research Award. The work of the second author was supported in part by the National Science Foundation under Grant No. DMS-06-52481. The work of the third author was supported in part by the National Science Foundation under Grant No. DMS-07-13835.

where $\boldsymbol{n}$ is the unit outer normal along $\partial\Omega$, and

$$H(\mathrm{div}^0;\Omega) = \Big\{\boldsymbol{v} \in [L_2(\Omega)]^2 : \nabla \cdot \boldsymbol{v} = \frac{\partial v_1}{\partial x_1} + \frac{\partial v_2}{\partial x_2} = 0\Big\}.$$

A related eigenproblem is to find $(\lambda, \mathring{\boldsymbol{u}}) \in \mathbb{R}\times[H_0(\mathrm{curl};\Omega)\cap H(\mathrm{div}^0;\Omega)]$ such that $\mathring{\boldsymbol{u}} \neq \mathbf{0}$ and

$$(1.2) \quad (\nabla \times \mathring{\boldsymbol{u}}, \nabla \times \boldsymbol{v}) = \lambda(\mathring{\boldsymbol{u}}, \boldsymbol{v}) \qquad \forall\, \boldsymbol{v} \in H_0(\mathrm{curl};\Omega) \cap H(\mathrm{div}^0;\Omega).$$

Since $H_0(\mathrm{curl};\Omega) \cap H(\mathrm{div}^0;\Omega)$ is compactly embedded in $[L_2(\Omega)]^2$ (cf. [20]), it follows from the Fredholm theory that (1.2) has nontrivial solutions for a sequence of nonnegative numbers (Maxwell eigenvalues) $\lambda_j$ $(j \geq 1)$ such that $\lambda_j \uparrow \infty$ as $j \uparrow \infty$. The problem (1.1) is well-posed if $\alpha \neq -\lambda_j$ for $j \geq 1$, and we assume this is the case throughout the paper. It is also easy to check that the strong (distributional) form of (1.1) is

$$(1.3) \qquad \nabla \times (\nabla \times \mathring{\boldsymbol{u}}) + \alpha\mathring{\boldsymbol{u}} = Q\boldsymbol{f},$$

where $Q$ is the orthogonal projection from $[L_2(\Omega)]^2$ onto $H(\mathrm{div}^0;\Omega)$.

The curl-curl problem (1.1) is related to the time-harmonic (frequency-domain) Maxwell equations when $\alpha \leq 0$ and the time-dependent (time-domain) Maxwell equations when $\alpha > 0$. Historically, since it is difficult to construct finite element spaces that are subspaces of $H_0(\mathrm{curl};\Omega) \cap H(\mathrm{div}^0;\Omega)$, the numerical solution of (1.1) has not been considered, even though $\nabla \cdot \mathring{\boldsymbol{u}} = 0$ is a desired feature in many electromagnetic problems. Instead, the curl-curl problem is posed on $H_0(\mathrm{curl};\Omega)$ and solved numerically by $H(\mathrm{curl};\Omega)$ conforming finite elements [35, 36, 11, 27, 32, 34]. See also [10, 5, 26, 3, 4, 22, 24, 19, 30, 31, 28, 29, 13, 12] for other approaches to the curl-curl problem.

In a recent paper [16], we solved (1.1) using the locally divergence-free weakly continuous $P_1$ vector fields of Crouzeix-Raviart [25] and techniques from discontinuous Galerkin methods. However, for a domain $\Omega$ that is not simply connected, the space of locally divergence-free weakly continuous $P_1$ vector fields does not have a completely local basis. To overcome this difficulty, we introduced in [15] an interior penalty method using locally divergence-free discontinuous $P_1$ vector fields. In this paper we consider a different approach: instead of giving up the weak continuity of the discrete vector fields, we abandon the locally divergence-free condition and replace it by a penalty term involving the local divergence of the weakly continuous $P_1$ vector fields. The analysis of the new scheme is greatly facilitated by its connections to the schemes in [16, 15].

The rest of the paper is organized as follows. We introduce the numerical scheme in Section 2, which is then analyzed in Section 3. Application to the Maxwell eigenproblem is discussed in Section 4. The results of numerical experiments are presented in Section 5, followed by some concluding remarks in Section 6.

## 2. The Numerical Scheme

Let $\mathcal{T}_h$ be a graded triangular mesh of $\Omega$ such that

$$h_T \approx h\Phi_\mu(T) \qquad \forall\, T \in \mathcal{T}_h, \tag{2.1}$$

where $h_T = \operatorname{diam} T$, $h = \max_{T\in\mathcal{T}} h_T$, and the weight $\Phi_\mu(T)$ is defined as follows:

$$\Phi_\mu(T) = \prod_{\ell=1}^{L} |c_\ell - c_T|^{1-\mu_\ell}. \tag{2.2}$$

Here $c_1, \ldots, c_L$ are the corners of $\Omega$, $c_T$ is the center of $T$, $\mu = (\mu_1, \ldots, \mu_L)$ is the vector containing the grading parameters, and the constants in the equivalence (2.1) are independent of $h$. Techniques for the construction of $\mathcal{T}_h$ can be found for example in [1, 2, 14, 8].

The following choice of the grading parameters is dictated by the behavior of the solution of (1.1):

$$\begin{aligned} \mu_\ell &= 1 && \text{if} \quad \omega_\ell \le \frac{\pi}{2}, \\ \mu_\ell &< \frac{\pi}{2\omega_\ell} && \text{if} \quad \omega_\ell > \frac{\pi}{2}, \end{aligned} \tag{2.3}$$

where $\omega_\ell$ is the interior angle at the corner $c_\ell$. In other words, grading is needed around any corner whose angle is larger than a right angle, which is different from the grading strategy for the Laplace operator, where grading is needed only around re-entrant corners. This is due to the fact that the singularity of the solution of (1.1) is one order more severe than the singularity of the solution of the Poisson problem for the Laplace operator [9, 6, 23, 21].

Let $V_h$ be the space of weakly continuous $P_1$ vector fields associated with $\mathcal{T}_h$ that respect the perfectly conducting boundary condition. More precisely,

$$\begin{aligned} V_h = \{\boldsymbol{v} \in [L_2(\Omega)]^2 :\ & \boldsymbol{v}_T = \boldsymbol{v}\big|_T \in [P_1(T)]^2\ \forall\, T \in \mathcal{T}_h, \boldsymbol{v} \text{ is continuous at} \\ & \text{the midpoints of the interior edges of } \mathcal{T}_h, \text{ and the tangential} \\ & \text{component of } \boldsymbol{v} \text{ vanishes at the midpoints of the boundary} \\ & \text{edges}\}. \end{aligned}$$

Since the discrete vector fields in $V_h$ are discontinuous in general, we need the piecewise curl and div operators defined by

$$(\nabla_h \times \boldsymbol{v})_T = \nabla \times \boldsymbol{v}_T \quad \text{and} \quad (\nabla_h \cdot \boldsymbol{v})_T = \nabla \cdot \boldsymbol{v}_T \quad \forall\, T \in \mathcal{T}_h, \tag{2.4}$$

and also take into account the tangential jump $[\![\boldsymbol{n} \times \boldsymbol{v}]\!]$ and normal jump $[\![\boldsymbol{n} \cdot \boldsymbol{v}]\!]$ of the discrete vector fields, which are defined as follows.

Let $e \in \mathcal{E}_h^i$ (the set of interior edges of $\mathcal{T}_h$) be shared by the triangles $T_{e,1}, T_{e,2} \in \mathcal{T}_h$ and $\boldsymbol{n}_1$ (resp. $\boldsymbol{n}_2$) be the unit normal of $e$ pointing towards the outside of $T_{e,1}$ (resp. $T_{e,2}$). We define on $e$

$$[\![\boldsymbol{n} \times \boldsymbol{v}]\!] = \boldsymbol{n}_1 \times \boldsymbol{v}_{T_{e,1}} + \boldsymbol{n}_2 \times \boldsymbol{v}_{T_{e,2}}, \tag{2.5a}$$

$$[\![\boldsymbol{n} \cdot \boldsymbol{v}]\!] = \boldsymbol{n}_1 \cdot \boldsymbol{v}_{T_{e,1}} + \boldsymbol{n}_2 \cdot \boldsymbol{v}_{T_{e,2}}. \tag{2.5b}$$

For an edge $e \in \mathcal{E}_h^b$ (the set of boundary edges of $\mathcal{T}_h$), we take $\boldsymbol{n}_e$ to be the unit normal of $e$ pointing towards the outside of $\Omega$ and define on $e$

$$[\![\boldsymbol{n} \times \boldsymbol{v}]\!] = \boldsymbol{n}_e \times \boldsymbol{v}. \tag{2.6}$$

The numerical scheme is: Find $\mathring{\boldsymbol{u}}_h \in V_h$ such that

$$a_h(\mathring{\boldsymbol{u}}_h, \boldsymbol{v}) = (\boldsymbol{f}, \boldsymbol{v}) \qquad \forall\, \boldsymbol{v} \in V_h, \tag{2.7}$$

where

$$\begin{aligned} a_h(\boldsymbol{w}, \boldsymbol{v}) &= (\nabla_h \times \boldsymbol{w}, \nabla_h \times \boldsymbol{v}) + h^{-2}(\nabla_h \cdot \boldsymbol{w}, \nabla_h \cdot \boldsymbol{v}) + \alpha(\boldsymbol{w}, \boldsymbol{v}) \\ &\quad + \sum_{e \in \mathcal{E}_h} \frac{[\Phi_\mu(e)]^2}{|e|} \int_e [\![\boldsymbol{n} \times \boldsymbol{w}]\!][\![\boldsymbol{n} \times \boldsymbol{v}]\!]\, ds \\ &\quad + \sum_{e \in \mathcal{E}_h^i} \frac{[\Phi_\mu(e)]^2}{|e|} \int_e [\![\boldsymbol{n} \cdot \boldsymbol{w}]\!][\![\boldsymbol{n} \cdot \boldsymbol{v}]\!]\, ds, \end{aligned} \tag{2.8}$$

$|e|$ denotes the length of the edge $e$, the weight $\Phi_\mu(e)$ is defined by

$$\Phi_\mu(e) = \prod_{\ell=1}^{L} |c_\ell - m_e|^{1-\mu_\ell}. \tag{2.9}$$

and $m_e$ denotes the midpoint of the edge $e$.

*Remark* 2.1. The two terms in (2.8) involving the jumps of the discrete vector fields across the edges are necessary for controlling the consistency error. The scheme without these terms is stable but not convergent (cf. the numerical results in Table 5.3 below). This is different from solving the Poisson problem for the Laplace operator by weakly continuous $P_1$ functions [18], where such terms are not needed. This is due to the fact that locally the norm of $H(\mathrm{Curl}) \cap H(\mathrm{div})$ is too weak to control the jumps even with the weak continuity of the vector fields in $V_h$.

*Remark* 2.2. The inclusion of the edge weight comes from the consideration of the regularity/singularity of $\mathring{\boldsymbol{u}}$ at the corners. The edge weight $\Phi_\mu(e)$ is closely related to the weight $\Phi_\mu(T)$ defined in (2.2). Indeed, we have

$$\Phi_\mu(e) \approx \Phi_\mu(T) \qquad \text{if} \quad e \subset \partial T, \tag{2.10}$$

where the constants in the equivalence depend only on the minimum angle in $\mathcal{T}_h$. The relation (2.10) plays an important role in ensuring optimal convergence in both the energy and the $L_2$ norm.

The advantage of using weakly continuous $P_1$ vector fields is due to the existence of a good interpolation operator $\Pi_h$ from $H_0(\text{curl};\Omega) \cap H(\text{div}^0;\Omega)$ into $V_h$. First we can define on each $T \in \mathcal{T}_h$ a local interpolation operator $\Pi_T : [H^s(T)]^2 \longrightarrow [P_1(T)]^2$ by the formula

$$(\Pi_T \boldsymbol{\zeta})(m_{e_i}) = \frac{1}{|e_i|} \int_{e_i} \boldsymbol{\zeta}\, ds \quad i = 1, 2, 3, \tag{2.11}$$

where $e_1$, $e_2$ and $e_3$ are the three edges of $T$. According to the trace theorem, the operator $\Pi_T$ is well-defined as long as $s > 1/2$. Moreover, we have the following interpolation estimate [25]:

$$\|\boldsymbol{\zeta} - \Pi_T\boldsymbol{\zeta}\|_{L_2(T)} + h_T^{\min(s,1)} |\boldsymbol{\zeta} - \Pi_T\boldsymbol{\zeta}|_{H^{\min(s,1)}(T)} \le C_T h_T^s |\boldsymbol{\zeta}|_{H^s(T)} \tag{2.12}$$

for all $\boldsymbol{\zeta} \in [H^s(T)]^2$ and $s \in (1/2, 2]$, where the positive constant $C_T$ depends on the minimum angle of $T$ (and also on $s$ when $s$ is close to $1/2$).

Since $H_0(\text{curl};\Omega) \cap H(\text{div}^0;\Omega)$ can be embedded into $[H^s(\Omega)]^2$ for some $s > 1/2$ (cf. e.g. [34]), we can piece together the local interpolation operator to define the global interpolation operator $\Pi_h$ by

$$(\Pi_h \boldsymbol{\zeta})_T = \Pi_T \boldsymbol{\zeta}_T \qquad \forall\, \boldsymbol{\zeta} \in H_0(\text{curl};\Omega) \cap H(\text{div}^0;\Omega),\ T \in \mathcal{T}_h.$$

Note that (2.11) implies $\Pi_h\boldsymbol{\zeta}$ is continuous at the midpoints of the interior edges of $\mathcal{T}_h$ and the tangential component of $\Pi_h\boldsymbol{\zeta}$ vanishes at the midpoints of the boundary edges. Hence $\Pi_h$ maps the space $H_0(\text{curl};\Omega) \cap H(\text{div}^0;\Omega)$ into $V_h$. Moreover it follows from the midpoint rule that

$$\int_e \Pi_T \boldsymbol{\zeta}\, ds = \int_e \boldsymbol{\zeta}\, ds$$

for any edge $e$ of $T \in \mathcal{T}_h$, which together with the Greens' theorem implies

$$\int_T \nabla \times (\Pi_T \boldsymbol{\zeta})\, dx = \int_T \nabla \times \boldsymbol{\zeta}\, dx \qquad \forall\, T \in \mathcal{T}_h,$$
$$\int_T \nabla \cdot (\Pi_T \boldsymbol{\zeta})\, dx = \int_T \nabla \cdot \boldsymbol{\zeta}\, dx \qquad \forall\, T \in \mathcal{T}_h.$$

This means, in view of (2.4), that

$$\Pi_0^h(\nabla\times\boldsymbol{\zeta}) = \nabla_h\times(\Pi_h\boldsymbol{\zeta}) \quad \text{and} \quad \Pi_0^h(\nabla\cdot\boldsymbol{\zeta}) = \nabla_h\cdot(\Pi_h\boldsymbol{\zeta}) \tag{2.13}$$

for all $\boldsymbol{\zeta}\in H_0(\text{curl};\Omega)\cap H(\text{div}^0;\Omega)$, where $\Pi_0^h$ is the $L_2$ orthogonal projection onto the space of piecewise constant functions associated with $\mathcal{T}_h$. The commutative relations in (2.13) indicate that we have good control for both the curl operator and the div operator, which explains why it is feasible to solve (1.1) using $V_h$.

## 3. Convergence Analysis

Since the scheme (2.7) is closely related to the schemes in [16] and [15], its convergence analysis can be carried out as in [16, 15] with only minor modifications.

We will measure the discretization error in both the $L_2$ norm and the mesh-dependent energy norm $\|\cdot\|_h$ defined by

$$\begin{aligned}\|\boldsymbol{v}\|_h^2 &= \|\nabla_h\times\boldsymbol{v}\|_{L_2(\Omega)}^2 + \|\boldsymbol{v}\|_{L_2(\Omega)}^2 + h^{-2}\|\nabla_h\cdot\boldsymbol{v}\|_{L_2(\Omega)}^2 \\ &\quad + \sum_{e\in\mathcal{E}_h}\frac{[\Phi_\mu(e)]^2}{|e|}\|[\![\boldsymbol{n}\times\boldsymbol{v}]\!]\|_{L_2(e)}^2 + \sum_{e\in\mathcal{E}_h^i}\frac{[\Phi_\mu(e)]^2}{|e|}\|[\![\boldsymbol{n}\cdot\boldsymbol{v}]\!]\|_{L_2(e)}^2.\end{aligned} \tag{3.1}$$

Observe that $a_h(\cdot,\cdot)$ is bounded by the energy norm:

$$a_h(\boldsymbol{w},\boldsymbol{v}) \le (1+|\alpha|)\|\boldsymbol{w}\|_h\|\boldsymbol{v}\|_h \qquad \forall\,\boldsymbol{v},\boldsymbol{w}\in H_0(\text{curl};\Omega)\cap H(\text{div}^0;\Omega)+V_h.$$

For $\alpha>0$, $a_h(\cdot,\cdot)$ is also coercive with respect to $\|\cdot\|_h$, i.e.,

$$a_h(\boldsymbol{v},\boldsymbol{v}) \ge \min(1,\alpha)\|\boldsymbol{v}\|_h^2 \qquad \forall\,\boldsymbol{v}\in[H_0(\text{curl};\Omega)\cap H(\text{div}^0;\Omega)]+V_h.$$

In this case the discrete problem is well-posed and we have the following abstract error estimate, whose proof is identical with the proof of Lemma 3.5 in [15].

**Lemma 3.1.** *Let $\alpha$ be positive, $\beta=\min(1,\alpha)$, $\mathring{\boldsymbol{u}}\in H_0(\text{curl};\Omega)\cap H(\text{div}^0;\Omega)$ be the solution of (1.1) and $\mathring{\boldsymbol{u}}_h\in V_h$ satisfy (2.7). It holds that*

$$\begin{aligned}\|\mathring{\boldsymbol{u}}-\mathring{\boldsymbol{u}}_h\|_h \le \Big(\frac{1+\alpha+\beta}{\beta}\Big)\inf_{\boldsymbol{v}\in V_h}\|\mathring{\boldsymbol{u}}-\boldsymbol{v}\|_h \\ + \frac{1}{\beta}\sup_{\boldsymbol{w}\in V_h\setminus\{\boldsymbol{0}\}}\frac{a_h(\mathring{\boldsymbol{u}}-\mathring{\boldsymbol{u}}_h,\boldsymbol{w})}{\|\boldsymbol{w}\|_h}.\end{aligned} \tag{3.2}$$

For $\alpha\le 0$, we have the following Gårding (in)equality:

$$a_h(\boldsymbol{v},\boldsymbol{v})+(|\alpha|+1)(\boldsymbol{v},\boldsymbol{v}) = \|\boldsymbol{v}\|_h^2 \qquad \forall\,\boldsymbol{v}\in[H_0(\text{curl};\Omega)\cap H(\text{div}^0;\Omega)]+V_h.$$

In this case the discrete problem is indefinite and the following lemma provides an abstract error estimate for the scheme (2.7) under the assumption that it has a solution. Its proof is identical with that of Lemma 3.6 in [15].

**Lemma 3.2.** *Let* $\mathring{\boldsymbol{u}} \in H_0(\mathrm{curl};\Omega) \cap H(\mathrm{div}^0;\Omega)$ *satisfy* (1.1) *and* $\mathring{\boldsymbol{u}}_h \in V_h$ *be a solution of* (2.7). *It holds that*

$$\|\mathring{\boldsymbol{u}} - \mathring{\boldsymbol{u}}_h\|_h \leq (2|\alpha|+3) \inf_{\boldsymbol{v}\in V_h} \|\mathring{\boldsymbol{u}} - \boldsymbol{v}\|_h + \sup_{\boldsymbol{w}\in V_h\setminus\{\boldsymbol{0}\}} \frac{a_h(\mathring{\boldsymbol{u}} - \mathring{\boldsymbol{u}}_h, \boldsymbol{w})}{\|\boldsymbol{w}\|_h} + (|\alpha|+1)\|\mathring{\boldsymbol{u}} - \mathring{\boldsymbol{u}}_h\|_{L_2(\Omega)}. \tag{3.3}$$

From here on we consider $\alpha$ to be fixed and drop the dependence on $\alpha$ in our estimates.

*Remark* 3.3. The first term on the right-hand sides of (3.2) and (3.3) measures the approximation property of the finite element space $V_h$, the second term measures the error due to the nonconforming nature of the scheme, and the third term on the right-hand side of (3.3) addresses the indefiniteness of (2.7) when $\alpha \leq 0$.

Since $\nabla \cdot \mathring{\boldsymbol{u}} = 0$ implies $\nabla_h \cdot (\Pi_h \mathring{\boldsymbol{u}}) = 0$ because of (2.13), we have

$$\begin{aligned}\|\mathring{\boldsymbol{u}} - \Pi_h\mathring{\boldsymbol{u}}\|_h^2 &= \|\mathring{\boldsymbol{u}} - \Pi_h\mathring{\boldsymbol{u}}\|_{L_2(\Omega)}^2 + \|\nabla_h \times (\mathring{\boldsymbol{u}} - \Pi_h\mathring{\boldsymbol{u}})\|_{L_2(\Omega)}^2 \\ &\quad + \sum_{e\in\mathcal{E}_h} \frac{[\Phi_\mu(e)]^2}{|e|} \|[\![\boldsymbol{n} \times (\mathring{\boldsymbol{u}} - \Pi_h\mathring{\boldsymbol{u}})]\!]\|_{L_2(e)}^2 \\ &\quad + \sum_{e\in\mathcal{E}_h^i} \frac{[\Phi_\mu(e)]^2}{|e|} \|[\![\boldsymbol{n} \cdot (\mathring{\boldsymbol{u}} - \Pi_h\mathring{\boldsymbol{u}})]\!]\|_{L_2(e)}^2.\end{aligned} \tag{3.4}$$

The terms on the right-hand side of (3.4) are identical with the terms that appear in the energy norm associated with the scheme in [16]. Therefore we have the following result on the approximation property of $V_h$, whose proof can be found in Lemma 5.1, Lemma 5.2 and Lemma 6.1 of [16].

**Lemma 3.4.** *Let* $\mathring{\boldsymbol{u}} \in H_0(\mathrm{curl};\Omega) \cap H(\mathrm{div}^0;\Omega)$ *be the solution of* (1.1). *For any* $\epsilon > 0$ *there exists a positive constant* $C_\epsilon$ *independent of* $h$ *and* $\boldsymbol{f}$ *such that*

$$\inf_{\boldsymbol{v}\in V_h} \|\mathring{\boldsymbol{u}} - \boldsymbol{v}\|_h \leq \|\mathring{\boldsymbol{u}} - \Pi_h\mathring{\boldsymbol{u}}\|_h \leq C_\epsilon h^{1-\epsilon}\|\boldsymbol{f}\|_{L_2(\Omega)}. \tag{3.5}$$

From here on we will use $C$ (with or without subscripts) to denote a generic positive constant independent of $h$ that can take different values at different appearances.

*Remark* 3.5. The proof of Lemma 3.4 is based on the regularity of the solution $\mathring{\boldsymbol{u}}$ of (1.1), the inclusion of the edge weight $\Phi_\mu(e)$ in (2.8), properties (2.12) and (2.13) of the interpolation operator $\Pi_h$, and properties (2.1) and (2.3) of the graded meshes $\mathcal{T}_h$. In [16] we focused on the case where $\alpha \leq 0$. Since the regularity of the solution $\mathring{\boldsymbol{u}}$ does not depend on the sign of $\alpha$, the results in [16] carry over to general $\alpha$.

Next we consider the consistency error, the analysis of which requires two preliminary estimates. The first one, which follows from the trace theorem with scaling, is identical with Lemma 5.3 in [16].

**Lemma 3.6.** *There exists a positive constant $C$ depending only on the shape regularity of $\mathcal{T}_h$ such that*

$$\sum_{e\in\mathcal{E}_h} |e|\,[\Phi_\mu(e)]^{-2}\|\eta-\bar{\eta}_{T_e}\|^2_{L_2(e)} \leq Ch^2|\nabla\eta|^2_{L_2(\Omega)} \qquad \forall\,\eta\in H^1(\Omega),$$

*where*

$$\bar{\eta}_{T_e} = \frac{1}{|T_e|}\int_{T_e}\eta\,dx$$

*is the mean of $\eta$ over $T_e$, one of the triangles in $\mathcal{T}_h$ that has $e$ as an edge.*

Recall that $Q$ is the $L_2$ orthogonal projection operator onto $H(\mathrm{div}^0;\Omega)$. The following result is useful in addressing the consistency error caused by the appearance of $Q$ in (1.3).

**Lemma 3.7.** *The following estimate holds*:

$$\|\boldsymbol{v}-Q\boldsymbol{v}\|_{L_2(\Omega)} \leq Ch\|\boldsymbol{v}\|_h \quad \forall\,\boldsymbol{v}\in[H_0(\mathrm{curl};\Omega)\cap H(\mathrm{div}^0;\Omega)]+V_h. \tag{3.6}$$

*Proof.* Let $\boldsymbol{v}\in[H_0(\mathrm{curl};\Omega)\cap H(\mathrm{div}^0;\Omega)]+V_h$ be arbitrary.

Since $\nabla H^1_0(\Omega)$ is the orthogonal complement of $H(\mathrm{div}^0;\Omega)$ in $[L_2(\Omega)]^2$, we have the following duality formula:

$$\begin{aligned}\|\boldsymbol{v}-Q\boldsymbol{v}\|_{L_2(\Omega)} &= \sup_{\eta\in H^1_0(\Omega)\setminus\{0\}}\frac{(\boldsymbol{v}-Q\boldsymbol{v},\nabla\eta)}{\|\nabla\eta\|_{L_2(\Omega)}}\\ &= \sup_{\eta\in H^1_0(\Omega)\setminus\{0\}}\frac{(\boldsymbol{v},\nabla\eta)}{\|\nabla\eta\|_{L_2(\Omega)}}.\end{aligned} \tag{3.7}$$

It follows from integration by parts and (2.5) that

$$(\boldsymbol{v},\nabla\eta) = -(\nabla_h\cdot\boldsymbol{v},\eta)+\sum_{e\in\mathcal{E}^i_h}\int_e [\![\boldsymbol{n}\cdot\boldsymbol{v}]\!]\eta\,ds. \tag{3.8}$$

In view of (3.1) and the Poincaré-Friedrichs inequality, we have

$$-(\nabla_h\cdot\boldsymbol{v},\eta) \leq \|\nabla_h\cdot\boldsymbol{v}\|_{L_2(\Omega)}\|\eta\|_{L_2(\Omega)} \leq Ch\|\boldsymbol{v}\|_h\|\nabla\eta\|_{L_2(\Omega)}. \tag{3.9}$$

Since $[\![\boldsymbol{n}\cdot\boldsymbol{v}]\!]$ vanishes at the midpoints of the interior edges, using the midpoint rule we can write

$$\sum_{e\in\mathcal{E}_h^i}\int_e [\![\boldsymbol{n}\cdot\boldsymbol{v}]\!]\eta\,ds = \sum_{e\in\mathcal{E}_h^i}\int_e [\![\boldsymbol{n}\cdot\boldsymbol{v}]\!](\eta-\bar{\eta}_{T_e})\,ds,$$

where $\bar{\eta}_{T_e}$ is the mean of $\eta$ on $T_e$, one of the triangles in $\mathcal{T}_h$ containing $e$ as an edge. It then follows from the Cauchy-Schwarz inequality, (3.1) and Lemma 3.6 that

$$\begin{aligned}\sum_{e\in\mathcal{E}_h^i}\int_e [\![\boldsymbol{n}\cdot\boldsymbol{v}]\!]\eta\,ds &\le \Big(\sum_{e\in\mathcal{E}_h^i}\frac{[\Phi_\mu(e)]^2}{|e|}\|[\![\boldsymbol{n}\cdot\boldsymbol{v}]\!]\|_{L_2(e)}^2\Big)^{1/2}\\ &\qquad\times\Big(\sum_{e\in\mathcal{E}_h^i}\frac{|e|}{[\Phi_\mu(e)]^2}\|\eta-\bar{\eta}_{T_e}\|_{L_2(e)}^2\Big)^{1/2}\\ &\le Ch\|\boldsymbol{v}\|_h\|\nabla\eta\|_{L_2(\Omega)}.\end{aligned}\tag{3.10}$$

The estimate (3.6) follows from (3.7)–(3.10). ☐

With Lemma 3.6 and Lemma 3.7 in hand, the following result is proved in exactly the same way as Lemma 6.2 of [16].

**Lemma 3.8.** *Let* $\mathring{\boldsymbol{u}}\in H_0(\text{curl};\Omega)\cap H(\text{div}^0;\Omega)$ *be the solution of* (1.1) *and* $\mathring{\boldsymbol{u}}_h\in V_h$ *satisfy* (2.7). *It holds that*

$$\sup_{\boldsymbol{w}\in V_h\setminus\{\boldsymbol{0}\}}\frac{a_h(\mathring{\boldsymbol{u}}-\mathring{\boldsymbol{u}}_h,\boldsymbol{w})}{\|\boldsymbol{w}\|_h}\le Ch\|\boldsymbol{f}\|_{L_2(\Omega)}.$$

Finally, we can establish the following $L_2$ estimate using a standard duality argument. The proof is identical with that of Lemma 6.5 in [16].

**Lemma 3.9.** *Let* $\mathring{\boldsymbol{u}}\in H_0(\text{curl};\Omega)\cap H(\text{div}^0;\Omega)$ *be the solution of* (1.1) *and* $\mathring{\boldsymbol{u}}_h\in V_h$ *satisfy* (2.7). *It holds that*

$$\|\mathring{\boldsymbol{u}}-\mathring{\boldsymbol{u}}_h\|_{L_2(\Omega)}\le C_\epsilon\big(h^{2-\epsilon}\|\boldsymbol{f}\|_{L_2(\Omega)}+h^{1-\epsilon}\|\mathring{\boldsymbol{u}}-\mathring{\boldsymbol{u}}_h\|_h\big)$$

*for any* $\epsilon>0$.

*Remark* 3.10. The fact that the problem (1.1) is posed for $\boldsymbol{f}\in[L_2(\Omega)]^2$ greatly simplifies the duality argument. In particular, the (continuous or discrete) Helmholtz decomposition is not needed.

In the case where $\alpha>0$, the following convergence theorem follows immediately from Lemma 3.1, Lemma 3.4, Lemma 3.8 and Lemma 3.9.

**Theorem 3.11.** *Let* $\alpha$ *be positive. The following estimates hold for the solution* $\mathring{\boldsymbol{u}}_h$ *of* (2.7):

$$\begin{aligned}\|\mathring{\boldsymbol{u}}-\mathring{\boldsymbol{u}}_h\|_h &\le C_\epsilon h^{1-\epsilon}\|\boldsymbol{f}\|_{L_2(\Omega)} &&\textit{for any}\quad \epsilon>0,\\ \|\mathring{\boldsymbol{u}}-\mathring{\boldsymbol{u}}_h\|_{L_2(\Omega)} &\le C_\epsilon h^{2-\epsilon}\|\boldsymbol{f}\|_{L_2(\Omega)} &&\textit{for any}\quad \epsilon>0.\end{aligned}$$

In the case where $\alpha \leq 0$, we have the following convergence theorem for the scheme (2.7). The proof, which is based on Lemma 3.2, Lemma 3.4, Lemma 3.8, Lemma 3.9 and the approach of Schatz [37] for indefinite problems, is identical with the proof of Theorem 4.5 in [15].

**Theorem 3.12.** *Assume that $-\alpha \geq 0$ is not a Maxwell eigenvalue. There exists a positive number $h_*$ such that the discrete problem* (2.7) *is uniquely solvable for all $h \leq h_*$, in which case the following discretization error estimates are valid*:

$$\|\mathring{\boldsymbol{u}} - \mathring{\boldsymbol{u}}_h\|_h \leq C_\epsilon h^{1-\epsilon} \|\boldsymbol{f}\|_{L_2(\Omega)} \qquad \text{for any} \quad \epsilon > 0,$$
$$\|\mathring{\boldsymbol{u}} - \mathring{\boldsymbol{u}}_h\|_{L_2(\Omega)} \leq C_\epsilon h^{2-\epsilon} \|\boldsymbol{f}\|_{L_2(\Omega)} \qquad \text{for any} \quad \epsilon > 0.$$

## 4. Application to the Maxwell Eigenproblem

We can find approximate solutions to the Maxwell eigenproblem (1.2) by solving the following discrete eigenproblem.

Find $(\lambda_h, \mathring{\boldsymbol{u}}_h) \in \mathbb{R} \times V_h$ such that $\mathring{\boldsymbol{u}}_h \neq \boldsymbol{0}$ and

$$a_{h,0}(\mathring{\boldsymbol{u}}_h, \boldsymbol{v}) = \lambda_h (\mathring{\boldsymbol{u}}_h, \boldsymbol{v}) \qquad \forall\, \boldsymbol{v} \in V_h, \tag{4.1}$$

where $a_{h,0}(\cdot,\cdot)$ is defined by (2.8) with $\alpha = 0$.

Let $T : [L_2(\Omega)]^2 \longrightarrow H_0(\text{curl};\Omega) \cap H(\text{div}^0;\Omega) \subset\subset [L_2(\Omega)]^2$ be the solution operator of the curl-curl problem define by

$$(\nabla \times T\boldsymbol{f}, \nabla \times \boldsymbol{v}) + (T\boldsymbol{f}, \boldsymbol{v}) = (\boldsymbol{f}, \boldsymbol{v})$$

for all $\boldsymbol{v} \in H_0(\text{curl};\Omega) \cap H(\text{div}^0;\Omega)$. Then $T$ is a symmetric positive compact operator on $[L_2(\Omega)]^2$ and $(\lambda, \mathring{\boldsymbol{u}}) \in \mathbb{R} \times [H_0(\text{curl};\Omega) \cap H(\text{div}^0;\Omega)]$ satisfies (1.2) if and only if

$$T\mathring{\boldsymbol{u}} = \frac{1}{1+\lambda}\mathring{\boldsymbol{u}}. \tag{4.2}$$

Similarly, let $T_h : [L_2(\Omega)]^2 \longrightarrow V_h \subset [L_2(\Omega)]^2$ be the discrete solution operator defined by

$$a_{h,1}(T_h\boldsymbol{f}, \boldsymbol{v}) = (\boldsymbol{f}, \boldsymbol{v}) \qquad \forall\, \boldsymbol{v} \in V_h,$$

where $a_{h,1}(\cdot,\cdot)$ is defined by (2.8) with $\alpha = 1$. Then $T_h$ is a symmetric finite rank operator and $(\lambda_h, \mathring{\boldsymbol{u}}_h) \in \mathbb{R} \times V_h$ satisfies (4.1) if and only if

$$T_h\mathring{\boldsymbol{u}}_h = \frac{1}{1+\lambda_h}\mathring{\boldsymbol{u}}_h. \tag{4.3}$$

It follows from Theorem 3.11 that

$$\|T\boldsymbol{f} - T_h\boldsymbol{f}\|_{L_2(\Omega)} \leq C_\epsilon h^{2-\epsilon} \|\boldsymbol{f}\|_{L_2(\Omega)} \qquad \forall\, \boldsymbol{f} \in [L_2(\Omega)]^2,\ \epsilon > 0. \tag{4.4}$$

Because of the uniform convergence of $T_h$ to $T$ described by (4.4), we can apply the classical theory of spectral approximation [33, 7] to prove the convergence of the eigenvalues (resp. eigenfunctions) of $T_h$ to the eigenvalues (resp. eigenfunctions) of $T$. The convergence of the eigenvalues (resp. eigenfunctions) of (4.1) to the eigenvalues (resp. eigenfunctions) of (1.2) then follows from (4.2) and (4.3). The proof of the following theorem is identical with the proof of Theorem 5.1 in [15].

**Theorem 4.1.** *Let* $0 \leq \lambda_1 \leq \lambda_2 \leq \dots$ *be the eigenvalues of* (1.2), $\lambda = \lambda_j = \lambda_{j+1} = \cdots = \lambda_{j+m-1}$ *be an eigenvalue with multiplicity* $m$, *and* $V_\lambda \subset H_0(\text{curl};\Omega) \cap H(\text{div}^0;\Omega)$ *be the corresponding* $m$ *dimensional eigenspace. Let* $\lambda_{h,1} \leq \lambda_{h,2} \leq \dots$ *be the eigenvalues of* (4.1). *Then, as* $h \downarrow 0$, *we have*

$$|\lambda_{h,\ell} - \lambda| \leq C_{\lambda,\epsilon} h^{2-\epsilon} \qquad \ell = j, \dots, j+m-1.$$

*Furthermore, if* $V_{h,\lambda} \subset V_h$ *is the space spanned by the eigenfunctions corresponding to* $\lambda_{h,j}, \dots, \lambda_{h,j+m-1}$, *then the gap between* $V_\lambda$ *and* $V_{h,\lambda}$ *goes to zero at the rate of* $C_\epsilon h^{2-\epsilon}$ *in the* $L_2$ *norm and at the rate of* $C_\epsilon h^{1-\epsilon}$ *in the norm* $\|\cdot\|_h$.

In particular, our scheme does not generate any spurious eigenmode.

## 5. Numerical Experiments

In this section we report the results of a series of numerical experiments that confirm our theoretical results. Besides the errors in the $L_2$ norm $\|\cdot\|_{L_2(\Omega)}$ and the energy norm $\|\cdot\|_h$, we also include the errors in the semi-norm $|\cdot|_{\text{curl}}$ defined by

$$|\boldsymbol{v}|_{\text{curl}} = \|\nabla_h \times \boldsymbol{v}\|_{L_2(\Omega)}$$

### 5.1. Source Problem.

We first demonstrate the performance of our scheme for the source problem in this subsection.

In the first experiment we examine the convergence behavior of our numerical scheme on the square domain $(0, 0.5)^2$ with uniform meshes, where the exact solution is

$$\mathring{\boldsymbol{u}} = [y(y-0.5)\sin(ky), x(x-0.5)\cos(kx)]. \tag{5.1}$$

The results are tabulated in Table 5.1 where $\alpha = k^2$ for $k = 0$, 1 and 10, and in Table 5.2 where $\alpha = -k^2$ for $k = 1$ and 10. They show that the method proposed in this paper is second order accurate in the $L_2$ norm and first order accurate in the energy norm, which agree with the error estimates in Theorem 3.11 and Theorem 3.12.

TABLE 5.1. Convergence of the scheme on the square $(0, 0.5)^2$ for $\alpha = k^2$, with uniform meshes and the exact solution given by (5.1).

| $h$ | $\frac{\|\mathring{\boldsymbol{u}} - \mathring{\boldsymbol{u}}_h\|_{L_2(\Omega)}}{\|\mathring{\boldsymbol{u}}\|_{L_2(\Omega)}}$ | order | $\frac{\|\mathring{\boldsymbol{u}} - \mathring{\boldsymbol{u}}_h\|_h}{\|\mathring{\boldsymbol{u}}\|_h}$ | order | $\frac{\lvert\mathring{\boldsymbol{u}} - \mathring{\boldsymbol{u}}_h\rvert_{\text{curl}}}{\lvert\mathring{\boldsymbol{u}}\rvert_{\text{curl}}}$ | order |
|---|---|---|---|---|---|---|
| $k = 0$ | | | | | | |
| 1/10 | 4.28E−02 | – | 2.89E−01 | – | 1.70E−01 | – |
| 1/20 | 9.68E−03 | 2.15 | 1.42E−01 | 1.02 | 8.52E−02 | 1.00 |
| 1/40 | 2.29E−03 | 2.08 | 7.05E−02 | 1.01 | 4.25E−02 | 1.00 |
| 1/80 | 5.56E−04 | 2.04 | 3.50E−02 | 1.00 | 2.12E−02 | 1.00 |
| $k = 1$ | | | | | | |
| 1/10 | 3.75E−02 | – | 2.70E−01 | – | 1.64E−01 | – |
| 1/20 | 8.46E−03 | 2.15 | 1.33E−01 | 1.02 | 8.14E−02 | 1.01 |
| 1/40 | 2.01E−03 | 2.08 | 6.60E−02 | 1.01 | 4.09E−02 | 1.00 |
| 1/80 | 4.86E−04 | 2.04 | 3.29E−02 | 1.01 | 2.05E−02 | 1.00 |
| $k = 10$ | | | | | | |
| 1/10 | 1.53E−01 | – | 6.49E−01 | – | 3.89E−01 | – |
| 1/20 | 3.49E−02 | 2.14 | 3.32E−01 | 0.97 | 1.97E−01 | 0.98 |
| 1/40 | 7.97E−03 | 2.13 | 1.66E−01 | 1.00 | 9.89E−02 | 0.99 |
| 1/80 | 1.90E−03 | 2.07 | 8.27E−02 | 1.00 | 4.93E−02 | 1.01 |

TABLE 5.2. Convergence of the scheme on the square $(0, 0.5)^2$ for $\alpha = -k^2$, with uniform meshes and the exact solution given by (5.1).

| $h$ | $\frac{\|\mathring{\boldsymbol{u}} - \mathring{\boldsymbol{u}}_h\|_{L_2(\Omega)}}{\|\mathring{\boldsymbol{u}}\|_{L_2(\Omega)}}$ | order | $\frac{\|\mathring{\boldsymbol{u}} - \mathring{\boldsymbol{u}}_h\|_h}{\|\mathring{\boldsymbol{u}}\|_h}$ | order | $\frac{\lvert\mathring{\boldsymbol{u}} - \mathring{\boldsymbol{u}}_h\rvert_{\text{curl}}}{\lvert\mathring{\boldsymbol{u}}\rvert_{\text{curl}}}$ | order |
|---|---|---|---|---|---|---|
| $k = 1$ | | | | | | |
| 1/10 | 3.83E−02 | – | 2.70E−01 | – | 1.64E−01 | – |
| 1/20 | 8.64E−03 | 2.15 | 1.33E−01 | 1.02 | 8.14E−02 | 1.00 |
| 1/40 | 2.04E−03 | 2.08 | 6.60E−02 | 1.01 | 4.09E−02 | 1.00 |
| 1/80 | 4.95E−04 | 2.04 | 3.29E−02 | 1.01 | 2.05E−02 | 1.00 |
| $k = 10$ | | | | | | |
| 1/10 | 3.69E−01 | – | 8.41E−01 | – | 4.07E−01 | – |
| 1/20 | 5.30E−02 | 2.80 | 3.46E−01 | 1.28 | 1.98E−01 | 1.04 |
| 1/40 | 1.13E−02 | 2.23 | 1.67E−01 | 1.05 | 9.89E−02 | 1.00 |
| 1/80 | 2.68E−03 | 2.08 | 8.27E−02 | 1.02 | 4.93E−02 | 1.00 |

In the second experiment we check the behavior of the scheme (2.7) without the consistency terms. The results in Table 5.3 show that these consistency terms are necessary for the convergence of the proposed scheme.

TABLE 5.3. Errors of the scheme without the consistency terms on the squares $(0, 0.5)^2$, with uniform meshes and the exact solution given by (5.1) with $k = 1$.

| $h$ | $\frac{\|\mathring{\boldsymbol{u}} - \mathring{\boldsymbol{u}}_h\|_{L_2(\Omega)}}{\|\mathring{\boldsymbol{u}}\|_{L_2(\Omega)}}$ | order | $\frac{\|\mathring{\boldsymbol{u}} - \mathring{\boldsymbol{u}}_h\|_{\text{curl}}}{\|\mathring{\boldsymbol{u}}\|_{\text{curl}}}$ | order |
|---|---|---|---|---|
| $\alpha = 1$ | | | | |
| 1/10 | 3.06E+01 | – | 4.66E−01 | – |
| 1/20 | 3.07E+01 | 0.00 | 4.51E−01 | 0.05 |
| 1/40 | 3.07E+01 | 0.00 | 4.48E−01 | 0.01 |
| 1/80 | 3.07E+01 | 0.00 | 4.46E−01 | 0.00 |
| $\alpha = -1$ | | | | |
| 1/10 | 3.06E+01 | – | 4.76E−01 | – |
| 1/20 | 3.07E+01 | 0.00 | 4.61E−01 | 0.04 |
| 1/40 | 3.07E+01 | 0.00 | 4.58E−01 | 0.01 |
| 1/80 | 3.07E+01 | 0.00 | 4.56E−01 | 0.00 |

The third experiment demonstrates the convergence behavior of our scheme on the $L$-shaped domain $(-0.5, 0.5)^2 \setminus [0, 0.5]^2$. The exact solution is chosen to be

$$\mathring{\boldsymbol{u}} = \nabla \times \left( r^{2/3} \cos\left(\frac{2}{3}\theta - \frac{\pi}{3}\right)\phi(r/0.5)\right), \tag{5.2}$$

where $(r, \theta)$ are the polar coordinates at the origin and the cut-off function is given by

$$\phi(r) = \begin{cases} 1 & r \le 0.25 \\ -16(r-0.75)^3 & \\ \quad \times \left[5 + 15(r-0.75) + 12(r-0.75)^2\right] & 0.25 \le r \le 0.75 \\ 0 & r \ge 0.75 \end{cases}$$

The meshes are graded around the re-entrant corner with the grading parameter equal to 1/3. The results are tabulated in Table 5.4 and they agree with the error estimates for our scheme. That is, the scheme is second order accurate in the $L_2$ norm and first order accurate in the energy norm.

*Remark* 5.1. In the case where $\alpha < 0$, the results of the experiments in this subsection are almost identical with those computed by the scheme in [16].

TABLE 5.4. Convergence of the scheme on the $L$-shaped domain $(-0.5, 0.5)^2\backslash[0, 0.5]^2$, with graded meshes and the exact solution given by (5.2).

| $h$ | $\frac{\|\mathring{\boldsymbol{u}} - \mathring{\boldsymbol{u}}_h\|_{L_2(\Omega)}}{\|\mathring{\boldsymbol{u}}\|_{L_2(\Omega)}}$ | order | $\frac{\|\mathring{\boldsymbol{u}} - \mathring{\boldsymbol{u}}_h\|_h}{\|\mathring{\boldsymbol{u}}\|_h}$ | order | $\frac{\lvert\mathring{\boldsymbol{u}} - \mathring{\boldsymbol{u}}_h\rvert_{\text{curl}}}{\lvert\mathring{\boldsymbol{u}}\rvert_{\text{curl}}}$ | order |
|---|---|---|---|---|---|---|
| $\alpha = 0$ | | | | | | |
| 1/4 | 9.85E+01 | – | 1.31E+01 | – | 4.94E−00 | – |
| 1/8 | 3.20E+01 | 1.62 | 6.50E−00 | 1.01 | 3.59E−00 | 0.46 |
| 1/16 | 3.27E−00 | 3.29 | 2.21E−00 | 1.56 | 7.79E−01 | 2.21 |
| 1/32 | 6.80E−01 | 2.26 | 1.09E−00 | 1.02 | 4.34E−01 | 0.84 |
| 1/64 | 1.65E−01 | 2.05 | 5.51E−01 | 0.99 | 2.34E−01 | 0.90 |
| $\alpha = 1$ | | | | | | |
| 1/4 | 7.53E+01 | – | 1.01E+01 | – | 3.52E−00 | – |
| 1/8 | 2.78E+01 | 1.44 | 5.87E−00 | 0.78 | 3.06E−00 | 0.20 |
| 1/16 | 3.20E−00 | 3.12 | 2.19E−00 | 1.42 | 7.74E−01 | 1.98 |
| 1/32 | 6.75E−01 | 2.24 | 1.09E−00 | 1.01 | 4.33E−01 | 0.84 |
| 1/64 | 1.61E−01 | 2.07 | 5.51E−01 | 0.99 | 2.34E−01 | 0.89 |
| $\alpha = -1$ | | | | | | |
| 1/4 | 1.44E+02 | – | 1.88E+01 | – | 7.77E−00 | – |
| 1/8 | 3.81E+01 | 1.92 | 7.40E−00 | 1.35 | 4.41E−00 | 0.82 |
| 1/16 | 3.35E−00 | 3.50 | 2.24E−00 | 1.73 | 7.87E−01 | 2.49 |
| 1/32 | 6.88E−01 | 2.28 | 1.09E−00 | 1.03 | 4.34E−01 | 0.86 |
| 1/64 | 1.71E−01 | 2.01 | 5.51E−01 | 0.99 | 2.34E−01 | 0.90 |

5.2. **Maxwell Eigenproblem.** In this subsection, we report numerical results for the Maxwell eigenproblem. In all of the plots, the symbol "o" on the right denotes the exact eigenvalue, and "(2)" indicates that the multiplicity of the eigenvalue is 2.

The first example concerns the eigenvalue problem on the square domain $(0, \pi)^2$. For this case, the exact eigenvalues are $r^2 + s^2$, $r, s = 0, 1, 2, 3, \cdots$, with $r^2 + s^2 \neq 0$. For instance, the first ten values are $1, 1, 2, 4, 4, 5, 5, 8, 9, 9$. The computation is performed with uniform meshes. Figure 5.1 shows the first twenty numerical eigenvalues versus the parameter $n = \pi/h$, and one can see the eigenvalues are well resolved even when the meshes are still coarse. Furthermore, the numerical eigenvalues are second order accurate (see Table 5.5) and there is no spurious eigenvalue.

In the second example, the eigenvalues for the $L$-shaped domain $(-0.5, 0.5)^2 \setminus [0, 0.5]^2$ are computed and the meshes are graded around

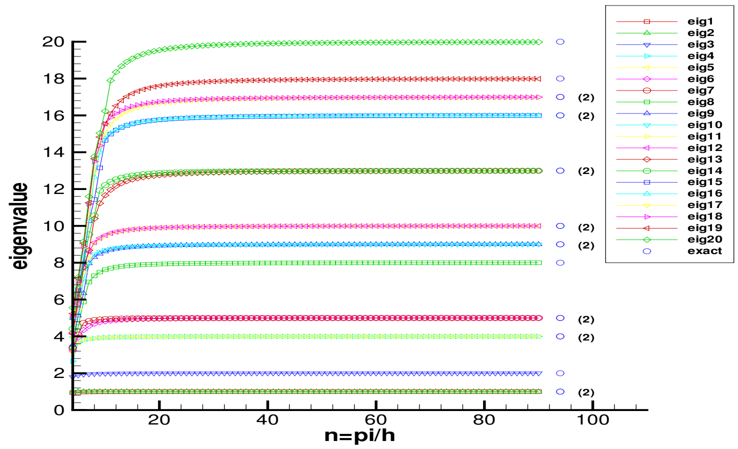


FIGURE 5.1. First twenty numerical Maxwell eigenvalues versus $n = \pi/h$ on the square $(0, \pi)^2$

TABLE 5.5. Convergence of the first five numerical Maxwell eigenvalues on the square $(0, \pi)^2$, with $\gamma$ = order of the convergence and $\lambda$ = exact eigenvalue

| $h/\pi$ | $1^{st}$ | $\gamma$ | $2^{nd}$ | $\gamma$ | $3^{rd}$ | $\gamma$ | $4^{th}$ | $\gamma$ | $5^{th}$ | $\gamma$ |
|---|---|---|---|---|---|---|---|---|---|---|
| $2^{-2}$ | 0.943 | - | 1.000 | - | 1.798 | - | 2.647 | - | 3.145 | - |
| $2^{-3}$ | 0.988 | 2.2 | 1.000 | - | 1.967 | 2.6 | 3.895 | 3.7 | 3.896 | 3.0 |
| $2^{-4}$ | 0.997 | 2.1 | 1.000 | 1.3 | 1.993 | 2.3 | 3.977 | 2.2 | 3.977 | 2.2 |
| $2^{-5}$ | 0.999 | 2.0 | 1.000 | 1.7 | 1.998 | 2.1 | 3.995 | 2.1 | 3.995 | 2.1 |
| $2^{-6}$ | 1.000 | 2.0 | 1.000 | 1.9 | 2.000 | 2.1 | 3.999 | 2.0 | 3.999 | 2.0 |
| $2^{-7}$ | 1.000 | 2.0 | 1.000 | 1.9 | 2.000 | 2.0 | 4.000 | 2.0 | 4.000 | 2.0 |
| $\lambda$ | 1 | | 1 | | 2 | | 4 | | 4 | |

the re-entrant corner with the grading parameter equal to 1/3. Table 5.6 contains the first five numerical eigenvalues which show second order convergence of our method. This agrees with our analysis. The "exact eigenvalues" in the table are derived from the Maxwell eigenproblem benchmark of Monique Dauge ( http://perso.univ-rennes1.fr/monique.dauge/core/index.html). In Figure 5.2, we plot the first ten numerical eigenvalues versus the parameter $n = 1/2h$. Again, there is no spurious eigenvalue.

TABLE 5.6. Convergence of the first five numerical Maxwell eigenvalues on the $L$-shaped domain $(-0.5, 0.5)^2 \setminus [0, 0.5]^2$ with graded meshes, $\mu = 1/3$ at the re-entrant corner, $\gamma$ = order of the convergence and $\lambda$ = exact eigenvalue

| $h$ | $1^{st}$ | $\gamma$ | $2^{nd}$ | $\gamma$ | $3^{rd}$ | $\gamma$ | $4^{th}$ | $\gamma$ | $5^{th}$ | $\gamma$ |
|---|---|---|---|---|---|---|---|---|---|---|
| $2^{-2}$ | 5.319 | - | 10.726 | - | 11.275 | - | 11.440 | - | 12.349 | - |
| $2^{-3}$ | 5.756 | 2.0 | 13.532 | 2.5 | 31.448 | 1.8 | 37.651 | 3.9 | 39.529 | 2.5 |
| $2^{-4}$ | 5.867 | 2.1 | 13.992 | 2.1 | 37.307 | 1.9 | 39.100 | 2.3 | 44.429 | 2.4 |
| $2^{-5}$ | 5.894 | 2.1 | 14.101 | 2.0 | 38.929 | 2.0 | 39.390 | 2.1 | 45.291 | 2.1 |
| $2^{-6}$ | 5.901 | 2.1 | 14.127 | 2.00 | 39.341 | 2.0 | 39.457 | 2.1 | 45.493 | 2.0 |
| $\lambda$ | 5.902 | | 14.136 | | 39.478 | | 39.478 | | 45.558 | |

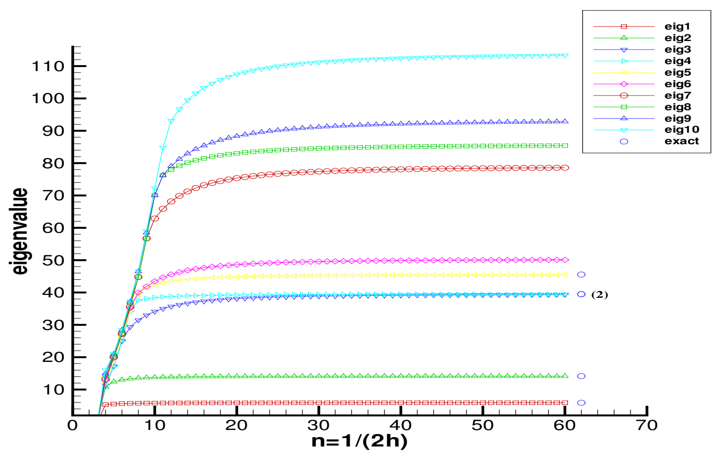


FIGURE 5.2. First ten numerical Maxwell eigenvalues versus $n = 1/2h$ on the $L$-shaped domain $(-0.5, 0.5)^2 \setminus [0, 0.5]^2$

## 6. Concluding Remarks

The numerical scheme in this paper is the third one we developed for the curl-curl problem posed on the space $H_0(\text{curl};\Omega) \cap H(\text{div}^0;\Omega)$. The scheme in [16] uses the smallest number of degrees of freedom ($\approx 2\times$number of triangles in $\mathcal{T}_h$), but the finite element space involved does not have a completely local basis when the domain is not simply connected. The scheme in the current paper uses a larger number of degrees of freedom ($\approx 3\times$number of triangles in $\mathcal{T}_h$), but it has a local basis for general domains. The scheme in [15] uses even more degrees of freedom ($\approx 5 \times$ number of triangles in $\mathcal{T}_h$), but it has a local basis for general domains and can also handle nonconforming meshes. All three schemes can be used in the computation of Maxwell eigenvalues without generating any spurious eigenmode. The numerical properties of these three schemes as Maxwell eigensolvers are further studied in [17].

The condition numbers of the discrete systems resulting from our schemes behave like the condition numbers of fourth order problems. It is therefore important to develop fast solvers for these methods. This is currently under investigation.

## References


[1] Th. Apel. *Anisotropic Finite Elements*. Teubner, Stuttgart, 1999.

[2] Th. Apel, A.-M. Sändig, and J.R. Whiteman. Graded mesh refinement and error estimates for finite element solutions of elliptic boundary value problems in non-smooth domains. *Math. Methods Appl. Sci.*, 19:63–85, 1996.

[3] F. Assous, P. Ciarlet, Jr., S. Labrunie, and J. Segré. Numerical solution to the time-dependent Maxwell equations in axisymmetric singular domains: the singular complement method. *J. Comput. Phys.*, 191:147–176, 2003.

[4] F. Assous, P. Ciarlet Jr., E. Garcia, and J. Segré. Time-dependent Maxwell's equations with charges in singular geometries. *Comput. Methods Appl. Mech. Engrg.*, 196:665–681, 2006.

[5] F. Assous, P. Ciarlet, Jr., S. Labrunie, and S. Lohrengel. The singular complement method. In N. Debit, M. Garbey, R. Hoppe, D. Keyes, Y. Kuznetsov, and J. Périaux, editors, *Domain Decomposition Methods in Science and Engineering*, pages 161–189. CIMNE, Barcelona, 2002.

[6] F. Assous, P. Ciarlet, Jr., P.-A. Raviart, and E. Sonnendrücker. Characterization of the singular part of the solution of Maxwell's equations in a polyhedral domain. *Math. Meth. Appl. Sci.*, 22:485–499, 1999.

[7] I. Babuška and J. Osborn. Eigenvalue Problems. In P.G. Ciarlet and J.L. Lions, editors, *Handbook of Numerical Analysis II*, pages 641–787. North-Holland, Amsterdam, 1991.

[8] C. Băcuţă, V. Nistor, and L.T. Zikatanov. Improving the rate of convergence of 'high order finite elements' on polygons and domains with cusps. *Numer. Math.*, 100:165–184, 2005.

[9] M. Birman and M. Solomyak. $L^2$-theory of the Maxwell operator in arbitrary domains. *Russ. Math. Surv.*, 42:75–96, 1987.

[10] A.-S. Bonnet-Ben Dhia, C. Hazard, and S. Lohrengel. A singular field method for the solution of Maxwell's equations in polyhedral domains. *SIAM J. Appl. Math.*, 59:2028–2044, 1999.

[11] A. Bossavit. *Computational Electromagnetism*. Academic Press, San Diego, 1998.

[12] J.H. Bramble, T.V. Kolev, and J.E. Pasciak. A least-squares approximation method for the time-harmonic Maxwell equations. *J. Numer. Math.*, 13:237–263, 2005.

[13] J.H. Bramble and J.E. Pasciak. A new approximation technique for div-curl systems. *Math. Comp.*, 73:1739–1762, 2004.
[14] S.C. Brenner and C. Carstensen. Finite Element Methods. In E. Stein, R. de Borst, and T.J.R. Hughes, editors, *Encyclopedia of Computational Mechanics*, pages 73–118. Wiley, Weinheim, 2004.
[15] S.C. Brenner, F. Li, and L.-Y. Sung. A locally divergence-free nonconforming finite element method for the time-harmonic Maxwell equations. *Math. Comp.*, 76:573–595, 2007.
[16] S.C. Brenner, F. Li, and L.-Y. Sung. A locally divergence-free interior penalty method for two dimensional curl-curl problems. *SIAM J. Numer. Anal.*, 46:1190–1211, 2008.
[17] S.C. Brenner, F. Li, and L.-Y. Sung. Nonconforming Maxwell eigensolvers. preprint, Department of Mathematics, Lousiana State University (http://www.math.lsu.edu/∼brenner/Eigen.pdf), 2008.
[18] S.C. Brenner and L.R. Scott. *The Mathematical Theory of Finite Element Methods* (*Second Edition*). Springer-Verlag, New York-Berlin-Heidelberg, 2002.
[19] P. Ciarlet, Jr. Augmented formulations for solving Maxwell equations. *Comput. Methods Appl. Mech. Engrg.*, 194:559–586, 2005.
[20] M. Costabel. A remark on the regularity of solutions of Maxwell's equations on Lipschitz domains. *Math. Methods Appl. Sci.*, 12:36–368, 1990.
[21] M. Costabel and M. Dauge. Singularities of electromagnetic fields in polyhedral domains. *Arch. Ration. Mech. Anal.*, 151:221–276, 2000.
[22] M. Costabel and M. Dauge. Weighted regularization of Maxwell equations in polyhedral domains. *Numer. Math.*, 93:239–277, 2002.
[23] M. Costabel, M. Dauge, and S. Nicaise. Singularities of Maxwell interface problems. $M^2AN$, 33:627–649, 1999.
[24] M. Costabel, M. Dauge, and C. Schwab. Exponential convergence of hp-FEM for Maxwell equations with weighted regularization in polygonal domains. *Math. Models Methods Appl. Sci.*, 15:575–622, 2005.
[25] M. Crouzeix and P.-A. Raviart. Conforming and nonconforming finite element methods for solving the stationary Stokes equations I. *RAIRO Anal. Numér.*, 7:33–75, 1973.
[26] C. Hazard and S. Lohrengel. A singular field method for Maxwell's equations: Numerical aspects for 2D magnetostatics. *SIAM J. Numer. Anal.*, 40:1021–1040, 2002.
[27] R. Hiptmair. Finite elements in computational electromagnetism. *Acta Numer.*, 11:237–339, 2002.
[28] P. Houston, I. Perugia, A. Schneebeli, and D. Schötzau. Interior penalty method for the indefinite time-harmonic Maxwell equation. *Numer. Math.*, 100:485–518, 2005.
[29] P. Houston, I. Perugia, A. Schneebeli, and D. Schötzau. Mixed discontinuous Galerkin approximation of of the Maxwell operator: the indefinite case. *M2AN*, 39:727–753, 2005.
[30] P. Houston, I. Perugia, and D. Schötzau. Mixed discontinuous Galerkin approximation of of the Maxwell opertor. *SIAM J. Numer. Anal.*, 42:434–459, 2004.

[31] P. Houston, I. Perugia, and D. Schötzau. Mixed discontinuous Galerkin approximation of of the Maxwell operator: non-stabilized formulation. *J. Sci. Comput.*, 22/23:315–346, 2005.
[32] J.-M. Jin. *The Finite Element Method in Electromagnetics* (*Second Edition*). John Wiley & Sons, Inc., New York, 2002.
[33] T. Kato. *Perturbation Theory of Linear Operators*. Springer-Verlag, Berlin, 1966.
[34] P. Monk. *Finite Element Methods for Maxwell's Equations*. Oxford University Press, New York, 2003.
[35] J.-C. Nédélec. Mixed finite elements in $\mathbf{R}^3$. *Numer. Math.*, 35:315–341, 1980.
[36] J.-C. Nédélec. A new family of mixed finite elements in $\mathbf{R}^3$. *Numer. Math.*, 50:57–81, 1986.
[37] A. Schatz. An observation concerning Ritz-Galerkin methods with indefinite bilinear forms. *Math. Comp.*, 28:959–962, 1974.

Center for Computation and Technology and Department of Mathematics, Louisiana State University, Baton Rouge, LA 70803
*E-mail address*: brenner@math.lsu.edu

Department of Mathematical Sciences, Rensselaer Polytechnic Institute, Troy, NY 12180
*E-mail address*: lif@rpi.edu

Department of Mathematics, Louisiana State University, Baton Rouge, LA 70803
*E-mail address*: sung@math.lsu.edu